The Madagascar Bloom – a serendipitous study

M.A. Srokosz & G.D Quartly

National Oceanography Centre, Southampton, SO14 3ZH, UK

(revised 12 September 2012)

[contact: mas@noc.ac.uk]

Abstract

The late austral summer (February-April) phytoplankton bloom that occurs east of Madagascar exhibits significant interannual variability and at its largest extent covers ~1% of the world's ocean surface area. The bloom raises many intriguing questions about how it begins, is sustained, propagates to the east, exports carbon and ends. It has been observed and studied using satellite ocean color observations, but the lack of *in situ* data makes it difficult to address these questions. Here we describe observations that were made serendipitously on a cruise in February 2005. These show clearly for the first time the simultaneous existence of a deep chlorophyll maximum at ~70-110 m depths (seen in SeaSoar fluorimeter data) and a surface chlorophyll signature (seen in SeaWiFS satellite ocean color data). The observations also show the modulation of biological signature at the surface by the eddy field, but not of the deep chlorophyll maximum. *Trichodesmium* dominates the bloom nearer to Madagascar, while the diatom *Rhizosolenia clevei* (and its symbiont *Richelia intracellularis*) dominates further from the island. The surface bloom seen in the SeaWiFS data is confined to the shallow (~30 m) mixed layer. It is hypothesized that the interannual variability in bloom intensity may be due to variations in coastal upwelling and thus the supply of iron, which is a micronutrient that can limit diazotroph growth.

1. Introduction

Longhurst [2001] was the first to describe the seasonal development of a major bloom east of Madagascar, using ocean color observations from space (from POLDER and SeaWiFS). He noted that the bloom typically occurred during the period February to April, but was not present every year. The data showed that blooms had occurred in 1997, 1999 and 2000. Lacking *in situ* observations Longhurst [2001] conjectured that the bloom was caused by the mixed layer deepening, a so-called entrainment bloom, but modulated by the presence of the eddy field. He speculated that the bloom might consist of nitrogen-fixing diazotrophic cyanobacteria *Trichodesmium*, but considered it more likely to be due to larger eukaryotic algal cells (entrainment hypothesis).

Srokosz et al. [2004] re-examined the bloom, also using ocean color data (OCTS and SeaWiFS data for September 1996 to March 2004), and found an additional bloom in 2002. They advanced an explanation for the rapid spread of the bloom to the east away from Madagascar based on the interplay of plankton growth and diffusion (due to the eddy field), leading to the propagation of a possible "plankton wave." Their study was limited to examining the mechanism for bloom propagation.

Uz [2007] studied the bloom using a combination of ocean color (SeaWiFS and MODIS), sea surface temperature (SST from AVHRR), *in situ* (Argo) and meteorological (re-analysis winds and wind stress curl, plus cyclone tracks) data. He discounted Longhurst's [2001] entrainment hypothesis and advanced a new hypothesis based on iron limitation. He conjectured that tropical cyclones causing heavy rain on Madagascar wash iron-rich sediments into the coastal waters. These are then spread eastward by eddy diffusion and trigger a nitrogen-fixing diazotroph bloom when shallow mixed layers form due to heating of the upper ocean. The interannual variability in the cyclone tracks – whether or not they make

43 landfall in Madagascar – is taken to explain the interannual variability of the bloom. Two
44 criticisms can be made of this hypothesis: first, Uz [2007] invokes the eddy diffusion
45 mechanism discussed by Srokosz et al. [2004] to explain the spread of iron eastwards. This
46 misses the key point of that paper; namely, that it is the combination of plankton growth and
47 eddy diffusion that allows the rapid eastward propagation of the bloom. For iron there is no
48 growth term and eddy diffusion is insufficient, on its own, to transfer material eastward
49 sufficiently fast to explain the bloom propagation. Second, the main rivers on Madagascar
50 drain to the west into the Mozambique Channel (as can be ascertained from an atlas), and
51 thus do not contribute to the waters within the East Madagascar Current. Furthermore, the
52 heavy rains associated with tropical cyclones occur mainly in northwest Madagascar and
53 would affect rivers flowing into the Mozambique Channel [Nassor & Jury, 1997, 1998].

54

55 In contrast to Uz [2007], Lévy et al. [2007] concluded that the bloom is due to upwelling at
56 the coast followed by transport to the east by the retroflection of the East Madagascar Current
57 (EMC; on the possible retroflection of the EMC see Quartly et al. [2006]; Siedler et al.
58 [2009]). Lévy et al. [2007] and Koné et al. [2009] consider the evolution of the bloom only
59 briefly, as part of a broader study of blooms in the Indian Ocean using SeaWiFS data and
60 coupled ocean physics and ecosystem model output. Neither study reproduces the
61 Madagascar bloom, primarily due to limitations of their biological models, though the spatial
62 resolutions of the models may also be inadequate, given the bloom is dominated by meso and
63 sub-mesoscale features, which the models do not resolve.

64 Wilson & Qiu [2008] have included the Madagascar bloom in their study of the global
65 distribution of summer chlorophyll blooms in oligotrophic gyres (defined by Wilson et al.
66 [2008], as chlorophyll > 0.15 mg m^{-3}). They note that this is the only such bloom that exhibits
67 eastward propagation (with the single exception of the 1997 bloom in the NE Pacific noted

by Wilson [2003]). They suggest that the bloom is influenced by "island mass effects," developing within the dynamic eddy field and current system emanating off the southern tip of Madagascar. In particular, they associate it with the existence of the South Indian Ocean Counter Current (SICC; Palastanga et al. [2007]), which would allow consistent eastward migration. This is problematical as the link between the currents near Madagascar and the SICC remains to be established from *in situ* observations. The paper also suggests that the bloom occurs at the edges of regions of *Trichodesmium* occurrence, and in an area of extremely low dust deposition (thus ruling out aeolian iron fertilization effects; as noted previously by Srokosz et al. [2004]). No explanation of the pronounced interannual variability of the Madagascar bloom is offered.

The study by Raj et al. [2010] makes use of satellite, model, re-analysis and hydrographic data and presents a large number of possible bloom mechanisms. Some of their explanations appear circular in that they use SeaWiFS data, output from a model that assimilates SeaWiFS data [Gregg, 2008] and estimates of *Trichodesmium* derived from SeaWiFS data [Westberry & Siegel, 2006] to support their view of the bloom. They conclude that *Trichodesmium* nitrogen fixers are involved in stimulating the bloom but, while mentioning the observations of Poulton et al. [2009], fail to note that these show that further to the east of Madagascar the dominant species is *Rhizosolenia clevei* (with symbiont *Richelia intracellularis*), while *Trichodesmium* are found mainly nearer to and to the south of Madagascar. They attribute the interannual variability of the bloom to a combination of upwelling, precipitation, light limitation and mesoscale eddies.

Most recently, Huhn et al. [2012] have applied Finite-Time Lyapunov Exponent and Finite-Time Zonal Drift analysis to altimetry-derived velocity fields south and east of Madagascar. Their results indicate the existence of eastward propagating jets, with the main jet at ~25˚S forming a meridional transport boundary so limiting the spread of the bloom northwards.

25˚S is a region of enhanced sea surface height variability, with eddy and / or Rossby wave propagation westward [Quartly et al., 2006]. The jet at 25˚S can potentially transport iron from south of Madagascar so fertilizing the bloom. The jet exists in non-bloom years and its interannual variability does not match that of the bloom, so this does not explain the latter behavior. Huhn et al. [2012] note that the plankton front propagates faster than the transport velocity of the jet.

Therefore, many outstanding question regarding the East Madagascar bloom remain unanswered: what are the causes of its significant interannual variability; what processes allow the bloom to occur in the oligotrophic gyre; and by what mechanisms is it initiated and terminated? Several hypotheses exist in the literature, as noted above, but there are few data available to test them.

This paper will not answer all the questions as the observations described below were obtained serendipitously! Rather, here the first combined physical, chemical and biological *in situ* observations of the bloom are reported (an earlier paper Poulton et al. [2009] focused on biological measurements from the same cruise). These serendipitous observations allow us to draw some conclusions and answer some questions about the bloom, specifically:

• what, if any, is the link between the surface bloom observed in ocean color data and the subsurface physics and biology, and how does this relate to the eddy structures?

• how deep does the surface bloom penetrate into the water column?

• how do the subsurface measurements relate to the surface ones of Poulton et al. [2009]?

2. MadEx cruise

From 26 January to 21 February 2005 a cruise (called MadEx) took place on the *RRS Discovery* that was aimed at studying the East Madagascar Current and its interaction with

116 the eddies to the south of Madagascar (see Figure 2(b) below for cruise region). Details of the
117 cruise, its objectives and the measurements made can be found in Quartly [2006]. The work
118 included the deployment of moorings, measurements made using SeaSoar, CTD casts, and
119 underway biological and chemical sampling from the ship's non-toxic underway seawater
120 supply (inlet depth at 5 m; see section 4). During the cruise, due to a medical emergency, it
121 was necessary to divert *RRS Discovery* to the island of Réunion. This "lost" 5 days from the
122 cruise program: 11 to 15 February. However, from satellite data, in particular ocean color
123 observations (see Figure 1 and section 3 below) that were being received on-board, it was
124 noted that a bloom to the east of Madagascar was present. Therefore, on the return journey
125 from Réunion, SeaSoar was deployed on 14 February to make measurements concurrent with
126 the underway sampling, thus giving the first (to our knowledge) *in situ* biological and
127 physical data on the bloom. The need to prepare SeaSoar instruments for deployment meant
128 that underway sampling from the ship's non-toxic underway seawater supply began earlier on
129 the return journey than the SeaSoar measurements. Due to the lost time, there was an urgent
130 need to return to the work area south of Madagascar and complete the planned cruise
131 program. This meant that it was not possible to stop and sample the bloom in more detail.
132 However, it did prove possible, without too much loss of time, to execute slight course
133 changes to allow the ship to pass through two eddies – one cyclonic and one anticyclonic (see
134 Figure 1) – as eddies are known to play a key role in the development of the bloom
135 [Longhurst, 2001]. The SeaSoar data described below cover the period 09.00 on 14 February
136 to 05.44 on 16 February, ~45 hours. As noted above, the underway biological and chemical
137 sampling started closer to Réunion and provided data hourly for macronutrients (nitrate,
138 phosphate, silicate) and chlorophyll-a during this period. Underway sampling for
139 phytoplankton species was more irregular.

Initial results for the phytoplankton species found in the surface waters, for the whole cruise, were published by Poulton et al. [2009]. They found that that the area to the south of Madagascar was dominated by *Trichodesmium*, while the bloom area to the east was dominated by *Trichodesmium* nearer to Madagascar but by diazotrophic diatoms (*Rhizosolenia clevei* with symbiont *Richelia intracellularis*) further to the east (see Figure 2 in Poulton et al. [2009]). This shows that nitrogen-fixers play an important role in the southwest Indian Ocean. Here the context of those observations, just for the bloom area, is examined by using a combination of physical, chemical and biological data from the cruise, in conjunction with satellite ocean color data.

3. Satellite observations

Figure 1(a) shows an ocean color composite image from SeaWiFS covering the period 14 to 17 February. It was a similar image received on board *RRS Discovery* that gave the first indication that that a bloom was present to the east of Madagascar. Overlaid on the image is that portion of the ship's track along which *in situ* observations were made using SeaSoar on the return from Réunion (see section 4 for the *in situ* observations). Figure 1(b) shows the corresponding altimetric absolute dynamic topography and the high and low correspond to the eddies seen in the SeaWiFS data that the ship passed through. Figure 1(c) shows the SST in which the warm East Madagascar Current (EMC) flowing to the southwest can be clearly seen as it leaves the Madagascar coast, and this corresponds to the lower chlorophyll values in Figure 1(a). The eddies that are evident in the SeaWiFS ocean color data and the absolute dynamic topography are difficult to discern in the SST (this was also the case when high resolution GHRSST data were examined – not shown). Enhanced surface chlorophyll levels occur around the periphery of both eddies which is consistent with advection away from a source near Madagascar, but could also be due to submesoscale processes at the periphery of eddies (cf. Calil & Richards [2010]).

In Figure 2 the development and decline of the bloom is seen in a sequence of 7-day composites of SeaWiFS ocean color images, covering the period from 12-18 January to 2-8 March 2005. As noted by Longhurst [2001], the development of the bloom is clearly modulated by the mesoscale eddy field that exists to the east of Madagascar. The enhanced chlorophyll on the shelf around Madagascar, as well as the low chlorophyll of the EMC (just offshore to the east of the island), are both evident. Another striking feature in Figure 2(d)-(h) is the cyclonic eddy that appears relatively stationary at around 50˚E, 26˚S. This is close to the location that was previously noted by Quartly et al. [2006] as a "parking place" for eddies, when their progression westward has halted for some (yet to be explained) reason. The *in situ* data were obtained during 14-16 February (see below) which overlaps the periods corresponding to Figure 2(e)&(f), the later stages of the 2005 bloom. In Figure 2(h) there is evidence of the spinning up of a cyclonic eddy inshore of the EMC, a phenomenon noted earlier by Machu et al. [2002].

As stated in the introduction, the bloom has previously been observed in satellite ocean color data, here we observed a bloom in 2005 in the *in situ* data. However, it should be noted that there is some variation in how different authors assess the existence or absence of the bloom in specific years. While there is agreement on the years when a strong bloom exists, there is disagreement as to whether a bloom is weak or does not happen. Uz [2007] gives a numerical criterion for the existence / non-existence of the bloom; based the ratio of the mean chlorophyll over the bloom area (defined as 24-33˚S, 48-66˚E) to the mean chlorophyll over an area further east (defined as 24-33˚S, 70-88˚E; see his Figure 2b). He states that the bloom was absent in 2005 and only weak filaments were observed. This might seem at odds with the assessment here, but Wilson & Qiu [2008] describe the bloom in 2005 as "not as well-developed" but their criterion for a late summer bloom is that chlorophyll is greater than 0.15 mg/m^3, which differs from that of Uz [2007]. Therefore, at the time of the cruise (February

2005) it can be concluded that there was a bloom, but it did not develop as far, was not as strong, and did not persist for as long, as those in strong bloom years (see the sequence of SeaWiFS images in Figure 10 of Wilson & Qiu [2008]).

One final point to note from Figure 2 is that, while there is some evidence for the eastward propagation of the bloom in 2005, this appears to happen in two somewhat separated regions. One region nearer to Madagascar ~47˚-60˚E (Figure 2a-f) and another further away ~65˚-70˚E (Figure 2d-h). It is not clear that the development of the bloom follows an orderly progression from west to east.

4. *In situ* observations

The data presented here from the MadEx cruise were obtained using underway sampling, ADCP (acoustic Doppler current profiler) and SeaSoar. The SeaSoar is a towed undulator and on this deployment carried standard CTD sensors that measured temperature and salinity, a fluorimeter that measured chlorophyll fluorescence, and an optical plankton counter (OPC) that is designed to provide data on the abundance (no. m^{-3}) and biovolume (mm^3 m^{-3}) of meso-zooplankton or particles in the size range 250-2000 μm. Here the data are analyzed in size classes 250-500, 500-1000, 1000-2000 μm. We present data only for 250-500 and 500-1000 μm, as the measurements get noisier with increasing size class, due to the size of the OPC aperture (5 cm x 2 cm). SeaSoar was towed at 8 knots (~4 m s^{-1}) making measurements down to depths of ~300-350 m. The data were binned and averaged and the results are presented on an 8 m by 5 km grid (5 km was chosen to ensure one up and down traverse by SeaSoar is included in each bin). For more details of the instruments and processing see Quartly [2006].

Figure 3 shows the sections for density, temperature, salinity, chlorophyll fluorescence, and biovolume along the return track from Réunion. Note that the fluorescence calibration is that

214 provided by the manufacturer and no attempt has been made to calibrate it against *in situ*
215 chlorophyll measurements due to the small amount of *in situ* data available (surface only and
216 none at depth). Therefore, the fluorescence data are used simply as a qualitative indicator of
217 chlorophyll. Clearly visible in the fluorescence (Figure 3e) is the deep chlorophyll maximum
218 (DCM) at around 70-110 m (mean depth ~93 m). At this depth the DCM will not be "seen"
219 by satellite ocean color sensors due to the attenuation of the signal by the water column
220 above (see da Silva et al. [2002] and Smith [1981]). Therefore, the signatures visible in the
221 satellite data (see Figure 1) must be due to very near surface phytoplankton chlorophyll that
222 the SeaSoar fluorimeter does not detect very well due to the quenching effects of sunlight.
223 Therefore, here we use the SeaWiFS surface chlorophyll observations rather than the SeaSoar
224 ones. SeaWiFS surface chlorophyll data along the SeaSoar track are also shown in Figure
225 3(h).

226 To examine the DCM more closely and to see whether it has any relationship to the eddies
227 that clearly modulate the surface chlorophyll (see Figure 1), the SeaSoar fluorescence with
228 density contours overlaid is plotted in Figure 4. Along the transect the DCM stays at a
229 relatively constant depth, between ~70-110 m, whereas the isopyncals change depth by as
230 much as ~150 m across the eddy features. There is also no clear relationship between the
231 chlorophyll levels in the DCM and the background eddy field. Similar plots for fluorescence
232 with temperature and salinity contours overlaid (not shown) also do not reveal any clear
233 relationship with the mesoscale (eddy) structures. This is true for both the intensity and depth
234 of the DCM.

235 The OPC biovolume data in size classes 250-500 and 500-1000 μm (Figure 3f & g) suggest
236 that the highest concentrations of particles are near the surface, in the top ~30 m, not at the
237 DCM. This could be because the OPC cannot measure microzooplankton (<250 μm) that
238 may be present in the vicinity of the DCM (it would "see" mesozooplankton >200 μm). By

examining vertical profiles of density, temperature and salinity (not shown) it was found that the mixed layer depth is ~30 m along the SeaSoar transect. This suggests that whatever is causing the signal in the OPC, mesozooplankton or something else (see discussion in section 5 below), is confined by summer stratification to the shallow mixed layer. The depth to which the increased biovolume and abundance are seen is roughly delimited by the 26.5˚C temperature contour (see Figure 3f&g). Neither salinity nor density gave such a clear delimitation of the increased biovolume and abundance.

The *RRS Discovery* has two hull-mounted ADCP (acoustic Doppler current profiler) instruments operating at 75 and 150 kHz, which allowed us to make underway measurements of the currents. Since the 75 kHz ADCP has greater depth penetration (~900 m) we show results from that instrument (with 16 m vertical and ~0.5 km along-track resolution; the latter corresponding to 2 minute sampling; see Quartly [2006]). Those obtained from the 150 kHz ADCP are similar, but only give data for the upper ~350 m of the water column. Figure 1(a) shows the surface currents, while Figure 3(d) shows the cross-track current component. These confirm the presence of the mesoscale eddies seen in the satellite data and show that the maximum velocities at the surface can reach ~1 ms^{-1}. The full-depth 75 kHz ADCP data (not shown) indicate that velocity structure penetrates down to at least 600 m for the cyclonic eddy (cf. Donohue & Toole [2003], Figure 10), while it seems to be confined more to the top 200 m for the anticyclonic one. In both cases the velocity structure penetrates much deeper than the DCM observed in the SeaSoar data.

During the cruise a number of satellite-tracked surface drifters, drogued at 15 m, were deployed. The tracks of two, one deployed prior to the diversion to Réunion and one deployed on the return leg, are shown in Figure 1(a) confirming the presence of the cyclonic and anticyclonic eddies evident in the SeaWiFS chlorophyll images and ADCP currents.

263 The cyclonic eddy centered ~(49.5˚E, 25.5˚S) is clearly discernible – doming up of
264 isopycnals – in the density, temperature and salinity observations at ~49.5-50.5˚E where the
265 SeaSoar track intersects the eddy (Figure 3). A simple calculation, based on the ADCP data
266 down to 600 m, shows a transport of 21.7 Sv to the east in the northern half of the eddy, and
267 17.7 Sv to the west in the southern half. Here, for the purpose of the calculation, the eddy is
268 delimited 48.8˚-50.6˚E in longitude, with center at 50.2˚E; but defining the edge is
269 problematical given that it is embedded in a complex flow field. Furthermore, the SeaSoar
270 track does not pass through the actual center of the eddy. Calculating the transport from 200-
271 600 m gives 12.9 Sv to the east and 12.4 Sv to the west, a more balanced result. As can be
272 seen from Figures 1 and 3(d), the flow near the surface (approximately the top 200m) is
273 intensified to the east.

274 The anticyclonic eddy, centered at ~(47.3˚E, 26.7˚S), is less discernible in the SeaSoar data
275 as it is more elongated in a southwest direction (Figure 1). This is due to the underlying
276 bathymetry and because satellite sea surface height data (not shown) suggest that it has
277 recently separated from a larger anticyclonic feature to the north. The strong currents at one
278 edge are clearly seen but are confined more to the top 200 m of the water column (Figure 3d).
279 The doming up and down of isopycnals is suggestive of an intra-thermocline eddy (ITE) as
280 found in the area previously by Nauw et al. [2006], but centered on a shallower depth ~100m,
281 rather than ~200 m as found Nauw et al. [2006]. However, the temperature and salinity
282 properties differ from those of the ITEs observed by Nauw et al. [2006] – here at 100m depth
283 they are ~23˚ and ~35.2, as compared to ~20˚ and ~35.8 at 200m [Nauw et al., 2006], so
284 warmer and fresher.

285 There is a subsurface salinity maximum of ~35.65 at depths of ~270 m at the northern end of
286 the SeaSoar track, shallowing to ~130 m and the deepening again to ~200 m at the
287 southwestern end (Figure 3c). In the cyclonic and anticyclonic eddies, the value of salinity at

288 the maximum and the depth of the maximum are similar to those found for cyclonic and
289 anticyclonic eddies in the Mozambique Basin by de Ruijter et al. [2004]. This indicates that
290 such eddies can cross the Madagascar Ridge from the east of Madagascar into the
291 Mozambique Basin (cf. Figure 9 of de Ruijter et al. [2004]).

292 To further examine the link between the SeaWiFS surface observations and the SeaSoar ones,
293 along-track surface chlorophyll values were taken from SeaWiFS data that were within 6.7
294 km of the locations of the gridded SeaSoar data (see Figure 5; given the resolution of the data
295 the choice of 6.7 km ensures that there will be at least one match up within the search radius).
296 While a comparison between the SeaWiFS and SeaSoar surface chlorophyll is not
297 informative, due to surface quenching affecting the SeaSoar fluorimeter data, a surprising
298 result was found when a comparison was made between SeaWiFS chlorophyll and biovolume
299 from the OPC. Figures 5 and 6 show that the SeaWiFS chlorophyll is well correlated with the
300 biovolume in the size classes 250-500 and 500-1000 μm (correlation coefficients of 0.78 and
301 0.76, respectively), which are also well correlated with each other (0.90). A similar result
302 holds for OPC abundances (0.79, 0.78, 0.94). These correlations are reminiscent of similar
303 ones found by Srokosz et al. [2003] during the North Atlantic spring bloom, where they were
304 indicative of predator-prey dynamics – phytoplankton being grazed by zooplankton and both
305 being eaten by larger zooplankton. Whether this is the explanation for what is observed here
306 will be considered further in the discussion below.

307 The biological and chemical sampling that was carried out on the cruise is fully described by
308 Poulton et al. [2009], so will only briefly be considered here, with a specific focus on the
309 samples taken along the SeaSoar transect. For biological and chemical analysis, water
310 samples were collected from the ship's non-toxic underway seawater supply (inlet depth 5 m)
311 every hour for measurements of chlorophyll-a and macronutrients (nitrate, phosphate,
312 silicate), and every 2–4 hours for large (>50 μm) diazotrophs. Diazotroph abundance was

313 measured on large volume (10 liter) water samples, which were slowly concentrated down to
314 ~20 ml by gentle removal of seawater through a 50 μm nylon mesh, and preserved with 2%
315 acidic Lugol's solution in 25 ml glass vials. The abundance of *Trichodesmium* colonies,
316 individual trichomes and diatom cells (per liter) were determined in the full preserved volume
317 using a 25 ml Bogorov tray and binocular microscope. Colonies of *Trichodesmium* were
318 converted into trichome numbers assuming each colony consisted of 200 trichomes (for more
319 details see Poulton et al. [2009] and Quartly [2006]).

320 Figure 5 shows the abundance of *Rhizosolenia* cells and *Trichodesmium* trichomes along the
321 transect. While there is some relationship between the *in situ* abundances and both the
322 SeaWiFS chlorophyll and OPC biovolume, there are insufficient numbers of *in situ* samples
323 to draw strong conclusions. Nevertheless, the observations are suggestive that SeaWiFS is
324 seeing the chlorophyll signature of *Rhizosolenia*, with its symbiont *Richelia*, and
325 *Trichodesmium*. Taken in conjunction with the results of Poulton et al. [2009, Figure 2] there
326 seems to be an indication that if *Trichodesmium* is present then *Rhizosolenia* is not and vice-
327 versa (though there is some overlap around 51˚E on the transect; Figure 5).

328 Figure 7 shows the SeaWiFS and *in situ* chlorophyll, together with nutrients (nitrate + nitrite,
329 silicate, phosphate) at the surface along the SeaSoar track. The SeaWiFS and *in situ*
330 chlorophyll show good agreement (mean difference, SeaWiFS minus *in situ*, of
331 -0.01 mg m^{-3}). Nitrate + nitrite and phosphate values are low, while silicate ones are not. The
332 low values of nitrate + nitrite are consistent with the presence of nitrogen fixers. Poulton et
333 al. (2009) noted that, over the whole cruise, the main areas of *Rhizosolenia* abundance were
334 associated with silicate concentrations < 1 μmol kg^{-1}, but Figures 5 and 7 suggest this is not
335 the case for the section of SeaSoar track studied here. Recollect that their paper presented
336 results from the whole cruise, whereas here the focus is only on the SeaSoar observations of

337 the bloom area, and the high abundances of *Rhizosolenia* found by Poulton et al. [2009] lie
338 beyond the end of the SeaSoar track further northeast towards Réunion.

339 There is a weak negative correlation (-0.50; data not shown) between the SeaWiFS surface
340 chlorophyll and the fluorescence at the DCM. Increased chlorophyll concentration at the
341 surface and the associated higher abundance of *Trichodesmium* or *Rhizosolenia* could both
342 lead to less light penetration to depth and so stronger light limitation and less chlorophyll at
343 the DCM. As the surface values of chlorophyll are low it is unlikely that the chlorophyll on
344 its own will affect the light levels at depth significantly, but the presence of higher
345 abundances of *Trichodesmium* or *Rhizosolenia* almost certainly will. In similar circumstances
346 Villareal et al. [2011] found a significant impact of diatoms on their transmissometer
347 measurements (a point that will recur in the discussion below).

348 5. Discussion

349 Having described the observations made during the cruise, we now turn to a consideration of
350 the possible explanations for what was observed.

351 ***5.1 DCM*** We have made the first observations of a DCM contemporaneous with a surface
352 Madagascar bloom. The depth of the DCM does vary along the SeaSoar transect (Figure 4)
353 and is probably set by the availability of light and the depth of the nitracline (recalling from
354 Figure 7 that the surface waters are depleted of nitrate). Unfortunately, there are no
355 subsurface nutrient measurements with which to verify this. With regard to light levels, a
356 simple calculation (following da Silva et al. [2002]), assuming a diffuse attenuation for light
357 of 0.05 m^{-1}, gives a euphotic (1% of surface light) depth of 92m, which is about the same
358 value as the mean depth of the DCM. The depth of the nitracline might be weakly modulated
359 by the presence of eddies (as found by Pidcock et al. [2010]), thus mesoscale structures might
360 influence the DCM indirectly but such an effect is not clearly seen in Figure 4. The DCM is

not visible in the OPC data, which suggests that it is dominated by different phytoplankton species to those forming the surface bloom. However, not having *in situ* water samples for the DCM means that it is not possible to be definitive on this point. Output from a global ecosystem model available at NOC (Yool et al. [2011]), for the location and time of year of the cruise, reveals the existence of a DCM but no surface bloom. In the model the DCM exists for most of the year, but seems to be disrupted by deeper mixing during the austral winter (July to September). The lack of a surface bloom in the model is unsurprising, as the ecosystem model does not include the nitrogen fixers that were observed on MadEx in the surface waters. The DCM SeaSoar observations and model results are consistent with what might be expected in the late summer for an ecosystem in an oligotrophic subtropical gyre, formed due to the phytoplankton's requirement for both nutrients and light.

5.2 Surface bloom It is unlikely that the OPC (see Figures 3, 5 and 6) is measuring the presence of mesozooplankton, as was the case in Srokosz et al's [2003] observations. As no zooplankton net sampling was possible, this cannot be proved conclusively. However, the size class 250-500 μm abundance (no. liter^{-1}; units chosen for ease of comparison with Poulton et al. [2009]) is in the range 0-12, while for the size class 500-1000 μm it is in the range 0-3. Poulton et al. [2009] suggest that each *Trichodesmium* colony contains about 200 trichomes. So from the *in situ* data in Figure 5 we estimate 0-2.5 *Trichodesmium* colonies per liter along with 0-200 diatom cells per liter. Poulton et al. [2009] also note that diatom dimensions were 200-800 μm by 40-60 μm (mean value 474 μm by 47 μm), so potentially detectable by the OPC. Given that *Trichodesmium* colonies can be of significant size O(mm) and that *Rhizosolenia* can also form assemblages or associations O(cm) (cf. Villareal et al. [2011] and references therein), the *in situ* and OPC estimates of abundance are not dissimilar. Therefore, most likely the OPC is giving some measure of the abundance of *Trichodesmium* and *Rhizosolenia* in the shallow mixed layer. As the high values of both OPC biovolume and

386 abundance are delimited in depth by the 26.5˚C isotherm, this is consistent with optimal
387 growth conditions for *Trichodesmium* and *Rhizosolenia*, as noted by Wilson & Qiu [2008]
388 and Breitbarth et al. [2007]. These observations show similarity to those of Villareal et al.
389 [2011]. In studying summer blooms of diatom-diazotroph assemblages (DDAs) in the North
390 Pacific gyre, they found that these could be seen clearly in transmissometer (optical) data but
391 did not have strong chlorophyll signatures. They defined a DDA bloom as abundances > 10^5
392 cells m^{-3}. Here, in the chlorophyll filaments (Figure 1 and 5) we have *Rhizosolenia*
393 abundances of up to 200 cells $liter^{-1}$ that is $2x10^5$ cells m^{-3}, which meets their criterion, with
394 even larger values further east (see Figure 2d of Poulton et al. [2009]). However, some
395 optical methods for counting colonies or DDAs could be sensitive to the effects of turbulent
396 flow, such as that which might be encountered at the OPC aperture as it is towed through the
397 water or in a pumped underway water sampling system. The turbulence could cause the
398 colonies or DDAs to break up, leading to uncertainty in the estimates of numbers and size.
399 One way to determine the actual number of colonies or assemblages would be to use an
400 instrument like the video plankton recorder, as was done in the Atlantic by Davis &
401 McGillicuddy [2006].

402 The observation that *Trichodesmium* are more abundant closer to Madagascar supports
403 Westberry & Siegel's [2006, Figure 3a&d] SeaWiFS (1998-2003) based estimates of how
404 often such blooms occur globally. Their estimates do not indicate the presence of
405 *Trichodesmium* further to the east but mainly to the south of and closer to but east of
406 Madagascar, consistent with Poulton et al's [2009] *in situ* observations. Poulton et al. [2009]
407 give estimates of the nitrogen fixation rates for the Madagascar bloom and show these are
408 significant (<0.5 mmol N m^{-2} day^{-1} for *Trichodesmium*, 0.4-2.4 mmol N m^{-2} day^{-1} for
409 diazoptrophic diatoms in the bloom region, comparable with estimates for other ocean
410 regions). The observations also cohere with the modeling of nitrogen fixers by Monteiro et al.

411 [2010, 2011], which show pronounced variability over a year in *Trichodesmium* and DDA
412 analogs to the east of Madagascar (Monteiro et al. [2010] Figure 3b&d), with the DDA
413 analogs showing great variability. Unfortunately, they do not indicate when during the year
414 that variability occurs, so it may or may not be at the time of the observed Madagascar
415 bloom. Monteiro et al. [2011, Figure 4 as compared to Figure 1a] show that the total
416 diazotroph biomass is increased east of Madagascar when they increase iron solubility in
417 their model. This suggests that iron might play a key role in the actual bloom. Note, however,
418 that the Monteiro et al. [2010, 2011] global model is of 1˚ x 1˚ spatial resolution so does not
419 capture the effects of the eddy field.

420 ***5.3 Causes of the bloom*** If the dominant species are nitrogen fixers could the Madagascar
421 bloom be being stimulated by the input of iron (potentially a limiting micronutrient) as
422 suggested by Uz(2007)? A recent review of aeolian iron deposition [Mahowald et al., 2009]
423 would suggest that this is too small in the Madagascar bloom region to significantly impact
424 phytoplankton growth through iron fertilization (< 0.01 g Fe m^{-2} yr^{-1}, as compared to Saharan
425 dust deposition in the Atlantic > 0.2 g Fe m^{-2} yr^{-1} which is known to have a fertilizing effect
426 [Marañón et al., 2010]). A more likely source of iron are the sediments in the shallower
427 waters on the continental shelf south of Madagascar which, if advected east, could cause the
428 bloom in a similar way that the blooms around Kerguelen [Blain et al., 2007] and Crozet
429 [Pollard et al., 2009] are formed. However, the strong interannual intermittency of the bloom
430 suggests that any release of iron from the sediments and into the surface waters must also be
431 strongly variable interannually (the Crozet bloom exhibits significant interannual variability
432 too; Pollard et al. [2007]). To the authors' knowledge, no data exist on the release of iron
433 from the sediments around Madagascar. Any release of iron from the sediments into the
434 surface waters could be related to the upwelling that occurs to the south of Madagascar,
435 which is thought to be variable interannually [DiMarco et al., 2000; Lutjeharms & Machu,

2000; Machu et al., 2002]. DiMarco et al. [2000] note that the upwelling depends on both the wind field and the behavior of the EMC, while Lutjeharms & Machu [2000] and Machu et al. [2002] show that that cyclonic eddy inshore of the EMC also affects the upwelling. As the upwelling variability is affected by the winds, the EMC and the eddy at the southern tip of Madagascar – none of which are sufficiently well understood individually nor well characterized by existing observations – their combined effects are even less certain. The transport of the iron to the east would be also be determined by the behavior of the eddy field and SICC [Srokosz et al., 2004; Palastanga et al., 2007; Huhn et al., 2012].

5.4 Eddies and the SICC For the cyclonic eddy there is a near surface (top 200m) intensification of the transport to the east relative to the west of about 4Sv. This occurs at about 25˚S, the latitude of the SICC [Palastanga et al., 2007; Huhn et al., 2012]. Nauw et al. [2008] estimate an SICC transport of 3 to 6Sv, while Huhn et al's [2012] SICC propagation speed of 0.14 m s^{-1} can be transformed into a transport estimate of 2.1 to 5.25Sv by assuming that the SICC has a width of 100 to 150km over a depth of 150 to 250m (based on Palastanga et al. [2007] Figure 5). Assuming the strengthening of the westward flow in the upper 200m of the eddy is caused by the presence of the SICC, the degree of intensification is consistent with these other estimates of SICC transport. However, this is an instantaneous transport estimate and the agreement with previous observations may be fortuitous given the intermittent nature of the SICC flow in a turbulent eddy field.

5.5 What limits the propagation of the bloom? Here the results of Mognin et al. [2009] for the Kerguelen bloom are suggestive. Essentially, the summer bloom depletes the iron advected from Kerguelen in the winter, at which point the bloom ceases. A similar scenario can be envisaged for the Madagascar bloom. Iron is upwelled from sediment near Madagascar and transported eastwards causing a bloom that lasts until the iron is exhausted. Interannual variability in the size of the bloom is caused by interannual variability in the

strength of the upwelling. Note that the advection of the iron would occur prior to the formation of the bloom and it would then be some other factor that gives the bloom its apparent eastward propagating behavior. Such an iron advection effect would be consistent with the results of Srokosz et al. [2004] and Huhn et al. [2012]. The presence of advected iron together with the shallowing of the mixed layer during the summer could lead to a bloom, as warm, stably stratified waters allow nitrogen fixers to flourish [Capone et al., 1997; Wilson & Qiu, 2008]. In 2005 (Figure 2) it is not clear that the bloom propagates eastward, as it occurs earlier at ~65˚E than at ~60˚E. Thus the bloom may develop by some combination of mixed layer shallowing and a mechanism that allows eastward propagation.

5.6 A possible scenario Pulling together the results of this and previous studies a potential scenario for the late summer Madagascar bloom emerges. The bloom is constituted of *Trichodesmium* and diatom-diazotroph assemblages, though not necessarily in coexistence. It may be fertilized by iron carried eastwards from the upwelling region south of Madagascar, with consumption of the iron ultimately limiting the spread of the bloom. It could be triggered by the warming and shallowing of the mixed layer in the summer, allowing nitrogen fixers to bloom. The interannual variability in the strength of the bloom would then be determined by variations in the strength of the upwelling from year-to-year. An outstanding challenge is to characterize the variability of the upwelling and see if it displays any relationship to the interannual intermittency of the bloom. A further challenge would be to determine whether iron flux from the sediments could support the bloom.

6. Conclusions

The exact mechanisms for the formation, propagation and extinction of the Madagascar bloom are still unclear, but the *in situ* observations from the MadEx cruise presented here and by Poulton et al. [2009] have clarified some aspects of the bloom. The only way to determine

485 the behavior of the complex biological, chemical and physical processes affecting the
486 Madagascar bloom would appear to be to mount a multi-year *in situ* observational program
487 that would capture both stronger and weaker bloom events and the beginning and end of the
488 bloom. It would also need to have a fuller biological, chemical and physical sampling
489 program than was possible on the cruise in 2005. For example, measurements of iron (in
490 water and potential aeolian deposition), water samples for phytoplankton species composition
491 at the surface and at the DCM, vertical zooplankton net hauls (also for species composition)
492 and direct determination of export flux are among the extra information that is required.

493 However, the data that were obtained serendipitously on the MadEx cruise allow the
494 following new insights into the bloom:

495 • a deep chlorophyll maximum (mean depth ~93 m) and a surface chlorophyll bloom are
496 found to exist simultaneously.

497 • the surface biological signature is modulated by the eddy field, but the deep chlorophyll
498 maximum does not seem to be.

499 • the surface bloom seen in ocean color data is confined to the shallow (~30 m) mixed layer.

500 • nitrogen fixers play a key role in the Madagascar blooms visible in satellite ocean color
501 data. *Trichodesmium* dominates near to Madagascar, while *Rhizosolenia/Richelia* dominates
502 further to the east, and both are detected by the OPC due to their organization into colonies
503 and assemblages.

504 • the surface bloom and the DCM are likely composed of different phytoplankton species, as
505 the OPC detects the former but not the latter.

506 These observations further our understanding of the bloom but, in agreement with Uz [2007],
507 we conclude that definitive determination nature of the bloom will require further and more
508 comprehensive *in situ* sampling to be carried out.

509

510 **Acknowledgements**

511 We would like to thanks the officers and crew of the *RRS Discovery*, the technical staff of the
512 National Marine Facilities and our fellow scientists for their hard work on the cruise. In
513 particular, our thanks go to our colleague John Allen for getting the best out of SeaSoar on
514 the cruise and processing much of the SeaSoar data. We are grateful to Alex Poulton and
515 Mark Stinchcombe for providing biological and chemical data from the cruise. SeaWiFS data
516 were obtained from NASA/GSFC, the Reynolds SST data from GHRSST, and sea surface
517 height from AVISO. NEODAAS provided near real-time satellite data during the cruise. We
518 are grateful for comments by reviewers on the paper that led to improvements in the revised
519 version.

520

521

References

Blain S. + 46 others 2007 Effect of natural iron fertilization on carbon sequestration in the Southern Ocean, *Nature*, **446**, 1070-1075.

Breitbarth E., Oschilies A. & LaRoche J. 2007 Physiological constraints on the global distribution of *Trichodesmium* – effect of temperature on diazotrophy, *Biogeosci*., **4**, 53-61.

Calil P.H.R. & Richards K.J. 2010 Transient upwelling hot spots in the oligotrophic North Pacific, *J. Geophys. Res*., **115**, doi:10.1029/2009JC005360.

Capone D.G., Zehr J.P., Paerl H.W., Bergman B. & Carpenter E.J. 1997 *Trichodesmium*, a globally significant marine cyanobacterium, *Science*, **276**, 1221-1229.

da Silva J.C.B., New A.L., Srokosz M.A. & Smyth T.J. 2002 On the observability of internal tidal waves in remotely-sensed ocean color data, *Geophys. Res. Lett*., **29**, doi:10.1029/2001GL013888.

Davis C.S. & McGillicuddy D.J. 2006 Transatlantic abundance of the N_2-fixing colonial cyanobacterium *Trichodesmium*, *Science*, **312**, 1517-1520.

de Ruijter W.P.M., van Aken H.M., Lutjeharms J.R.E., Mantano R.P. & Schouten M.W. 2004 Eddies and diploes around South Madagascar: formation, pathways and large-scale impacts, *Deep-Sea Res. I*, **51**, 383-400.

DiMarco S.F., Chapman P. & Nowlin W.D. 2000 Satellite observations of upwelling on the continental shelf south of Madagascar, *Geophys. Res. Lett*., **27**, 3965-3968.

Donohue K.A. & Toole J.M. 2003 A near-synoptic survey of the Southwest Indian Ocean, *Deep-Sea Res*., **50**, 1893-1931.

544 Gregg W.W. 2008 Assimilation of SeaWiFS ocean chlorophyll data into a three-dimensional
545 global ocean model, *J. Mar. Sys*., **69**, 205-225.

546 Huhn F., von Kameke A., Pérez-Muñuzuri V., Olascoaga M.J. & Beron-Vera F.J. 2012 The
547 impact of advective transport by the South Indian Ocean Countercurrent on the
548 Madagascar bloom, *Geophys. Res. Lett*., **39**, doi:10.1029/2012GL051246.

549 Koné V, Aumont O., Lévy M. & Resplandy L. 2009 Physical and biogeochemical controls of
550 the phytoplankton seasonal cycle in the Indian Ocean: a modeling study, pp.147-166 in
551 Indian Ocean Biogeochemical Processes and Ecological Variability, *Geophys. Mono.*
552 *Ser.* **185**, AGU, Washington DC.

553 Lévy M., Shankar D., André J.-M., Shenoi S.S.C., Durand F. & de Boyer Montégut C. 2007
554 Basin-wide seasonal evolution of the Indian Ocean's phytoplankton blooms, *J.*
555 *Geophys. Res.*, **112**, C12014, doi:10.1029/2007JC004090.

556 Longhurst, A. 2001 A major seasonal phytoplankton bloom in the Madagascar Basin. *Deep-*
557 *Sea Res. I,* **48,** 2413-2422.

558 Lutjeharms J.R.E. & Machu E. 2000 An upwelling cell inshore of the East Madagascar
559 Current, *Deep-Sea Res. I*, **47**, 2405-2411.

560 Machu E., Lutjeharms J.R.E., Webb A.M. & van Aken H. 2002 First hydrographic evidence
561 of the southeast Madagascar upwelling cell, *Geophys. Res. Lett*., **29**,
562 doi:10.1029/2002GL0015381.

563 Mahowald N.M. + 19 others 2009 Atmospheric dust deposition: global distribution,
564 variability and human perturbations, *Ann. Rev. Mar. Sci*. **1**, 245-278.

565 Marañón E. + 15 others 2010 Degree of oligotrophy controls the response of microbial
566 plankton to Saharan dust, *Limnol. Oceanogr*., **55**, 2339-2352.

567 Mognin M.M., Abraham E.R. & Trull T.W. 2009 Winter advection of iron can explain the
568 summer phytoplankton bloom that extends 1000km downstream of the Kerguelen
569 Plateau in the Southern Ocean, *J. Mar. Res*., **67**, 225-237.

570 Monteiro F.M., Follows M.J. & Dutkiewicz S. 2010 Distribution of diverse nitrogen fixers in
571 the global ocean, *Global Biogeochem. Cyc*., **24**, doi:10.1029/2010GB003902.

572 Monteiro F.M., Follows M.J. & Dutkiewicz S. 2011 Biogeographical controls on the marine
573 nitrogen fixers, *Global Biogeochem. Cyc*., **25**, doi:10.1029/2009GB0037331.

574 Nassor A. & Jury M.R. 1997 Intra-seasonal climate variability of Madagascar. Part 2:
575 evolution of flood events, *Meteorol. Atmos. Phys.*, **64**, 243-254.

576 Nassor A. & Jury M.R. 1998 Intra-seasonal climate variability of Madagascar. Part 1: mean
577 summer conditions, *Meteorol. Atmos. Phys.*, **65**, 31-41.

578 Nauw, J.J., van Aken, H.M., Lutjeharms, J.R.E., de Ruijter, W.P.M., 2006 Intrathermocline
579 eddies in the Southern Indian Ocean. *J. Geophys. Res.*, **111**, C03006,
580 doi:10.1029/2005JC002917.

581 Nauw, J.J., van Aken, H.M., Lutjeharms, J.R.E., de Ruijter, W.P.M., 2008 Observations of
582 the southern East Madagascar Current and undercurrent and countercurrent system. *J.*
583 *Geophys. Res.*, **113**, C08006, doi:10.1029/2007JC004639.

584 Palastanga V., van Leeuwen P.J., Schouten M.W. & de Ruijter W.P.M. 2007 Flow structure
585 and variability in the subtropical Indian Ocean: instability of the South Indian Counter
586 Current, *J. Geophys. Res.*, **112**, C01001, doi:10.1029/2005JC003395.

587 Pidcock R., Srokosz M., Allen J., Hartman M., Painter S., Mowlem M., Hydes D. & Martin
588 A. 2010 A Novel Integration of an Ultra-Violet Nitrate Sensor On-Board A Towed
589 Vehicle for Mapping Open Ocean Submesoscale Nitrate Variability, *J. Atmos. Oceanic.*
590 *Tech.*, **27**, 1410-1416.

591 Pollard R., Sanders R., Lucas M. & Statham P. 2007 The Crozet natural iron bloom and
592 export experiment, *Deep-Sea Res. II*, **54**, 1905-1914.

593 Pollard, R.T. + 35 others 2009 Southern Ocean deep-water carbon export enhanced by
594 natural iron fertilization, *Nature*, **457**, 577-581.

595 Poulton A.J., Stinchcombe M.C. & Quartly G.D. 2009 High numbers of *Trichodesmium* and
596 diazotrophic diatoms in the southwest Indian Ocean, *Geophys. Res. Lett*., **36**, L15610,
597 doi:10.1029/2009GL0397179.

598 Quartly G.D. 2006 Madagascar Experiment (MadEx), RRS Discovery Cruise 288, 26 Jan –
599 21 Feb 2005, Cruise Report No. 8, National Oceanography Centre, Southampton,
600 105pp (available at http://eprints.soton.ac.uk/42070/).

601 Quartly G.D., Buck J.J.H., Srokosz M.A. & Coward A.C 2006 Eddies around Madagascar –
602 the retroflection re-considered, *J. Mar. Sys.*, **63**, 115-129.

603 Reynolds R.W., Smith T.M., Liu C., Chelton D.B., Casey K.S. & Schlax M.G. 2007 Daily
604 high-resolution-blended analyses for sea surface temperature, *J. Clim*., **20**, 5473-5492,
605 doi: 10.1175/2007JCLI1824.1

606 Raj R.P., Peter B.N. & Pushadas D. 2010 Oceanic and atmospheric influences on the
607 variability of phytoplankton bloom in the Southwestern Indian Ocean, *J. Mar. Sys*., **82**,
608 217-229.

609 Siedler G., Rouault M. Biastoch A. Backeberg E., Reason C.J.C. & Lutjeharms J.R.E. 2009
610 Modes of the southern extension of the East Madagascar Current, *J. Geophys*. Res.,
611 **114**, C01005, doi:10.1029/2008JC004921.

612 Smith R.C. 1981 Remote sensing and the depth distribution of ocean chlorophyll, *Mar. Ecol.*
613 *– Prog. Ser*., **5**, 359-361.

614 Srokosz M.A., Martin A.P. & Fasham M.J.R. 2003 On the role of biological dynamics in
615 plankton patchiness at the mesoscale: an example from the eastern North Atlantic
616 Ocean, *J. Mar Res*., **61**, 517-537.

617 Srokosz M.A., Quartly G.D. & Buck J.J.H. 2004 A possible plankton wave in the Indian
618 Ocean, *Geophys. Res. Lett*., **31**, L13301, doi:10.1029/2004GL109738.

619 Uz, B.M. 2007 What causes the sporadic phytoplankton bloom southeast of Madagascar? *J.*
620 *Geophys. Res.*, **112**, C09010, doi:10.1029/2006JC003685.

621 Villareal T.A., Adornato L., Wilson C. & Schoenbaechler C.A. 2011 Summer blooms of
622 diatom-diazotroph assemblages and surface chlorophyll in the North Pacific gyre: a
623 disconnect, *J. Geophys. Res*., **116**, C03001, doi:10.1029/2010JC006268.

624 Westberry T.K. & Siegel D.A. 2006 Spatial and temporal distribution of *Trichodesmium*
625 blooms in the world's ocean, *Global Biogeochem. Cycles*, **20**, GB4016,
626 doi:10.1029/2005GB002673.

627 Wilson C. 2003 Late summer chlorophyll blooms in the oligotrophic North Pacific
628 Subtropical Gyre, *Geophys. Res. Lett*., **30**, 1942, doi:10.1029/2003GL017770.

629 Wilson C., Villareal T.A., Maximenko N., Bograd S.J., Montoya J.P. & Schoenbaechler C.A.
630 2008 Biological and physical forcings of late summer chlorophyll blooms at 30˚N in
631 the oligotrophic Pacific, *J. Mar. Sys*., **69**, 164-176.

632 Wilson C. & Qiu X. 2008 Global distribution of summer chlorophyll blooms in the
633 oligotrophic gyres, *Prog. Oceanogr*., **78**, 107-134.

634 Yool A., Popova E.E. & Anderson T.R. 2011 MEDUSA-1.0: a new intermediate complexity
635 plankton ecosystem model for the global domain, *Geosci. Model Dev*., **4**, 381–417.

636

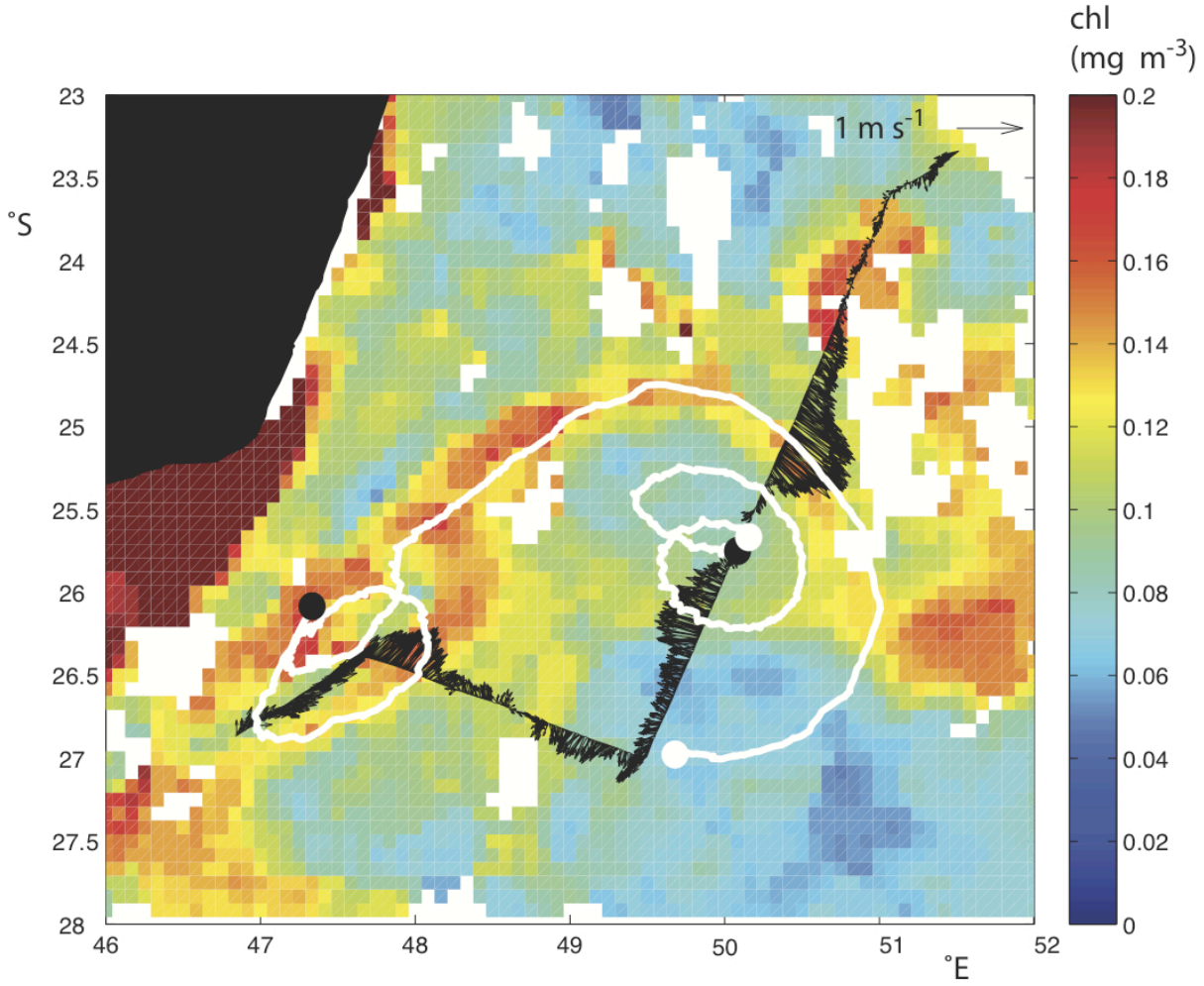

Figure 1a Ocean color composite image for 14 to 17 February 2005. Four daily 9 km resolution SeaWiFS datasets are combined using the mean of their logarithms to avoid sensitivity to extreme high values. The track of the *RRS Discovery* is overlaid with its 75kHz ADCP surface currents (in black), plus the trajectories of two satellite-tracked surface drifters (drogued at 15m) deployed during the cruise. The track of the buoy deployed in the cyclonic eddy is for 20 days after deployment from the ship, while the track for the buoy in the anticyclonic eddy (deployed earlier in the cruise) is from 10 days prior to ship's passage to 20 days afterwards. Black dots mark the start of drifter tracks, white dots the end. The scale arrow represents a flow of 1 m s^{-1}.

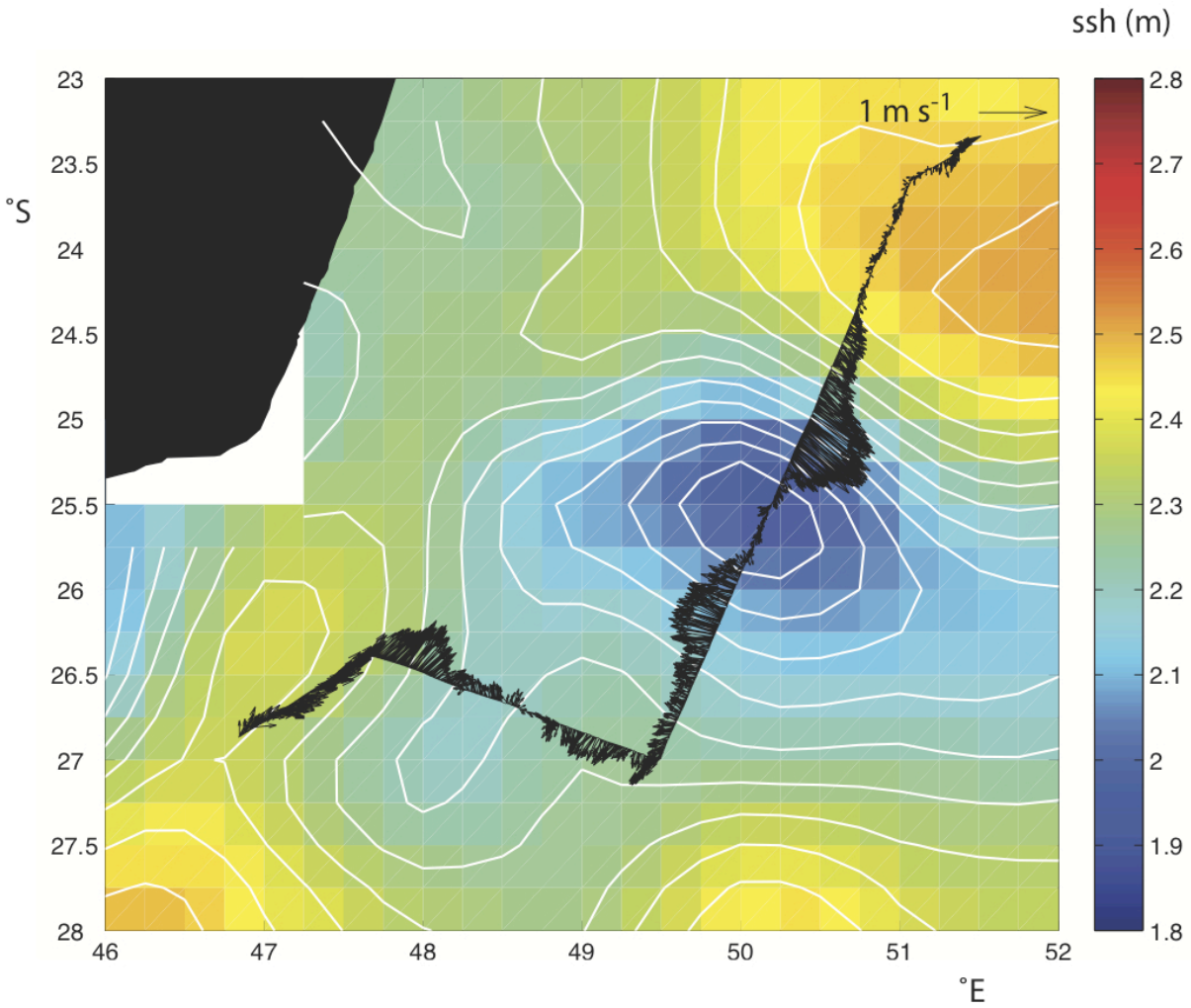

Figure 1b Absolute dynamic height from altimetry, with height contours superimposed (every 5cm), for the week centered on the 16th February 2005. Data used are from AVISO's DUACS 0.25° "update" product, which uses all altimeter data available for that period. As in a) the 75kHz ADCP surface currents are overlaid (in black), with scale arrow representing a flow of 1 m s^{-1}.

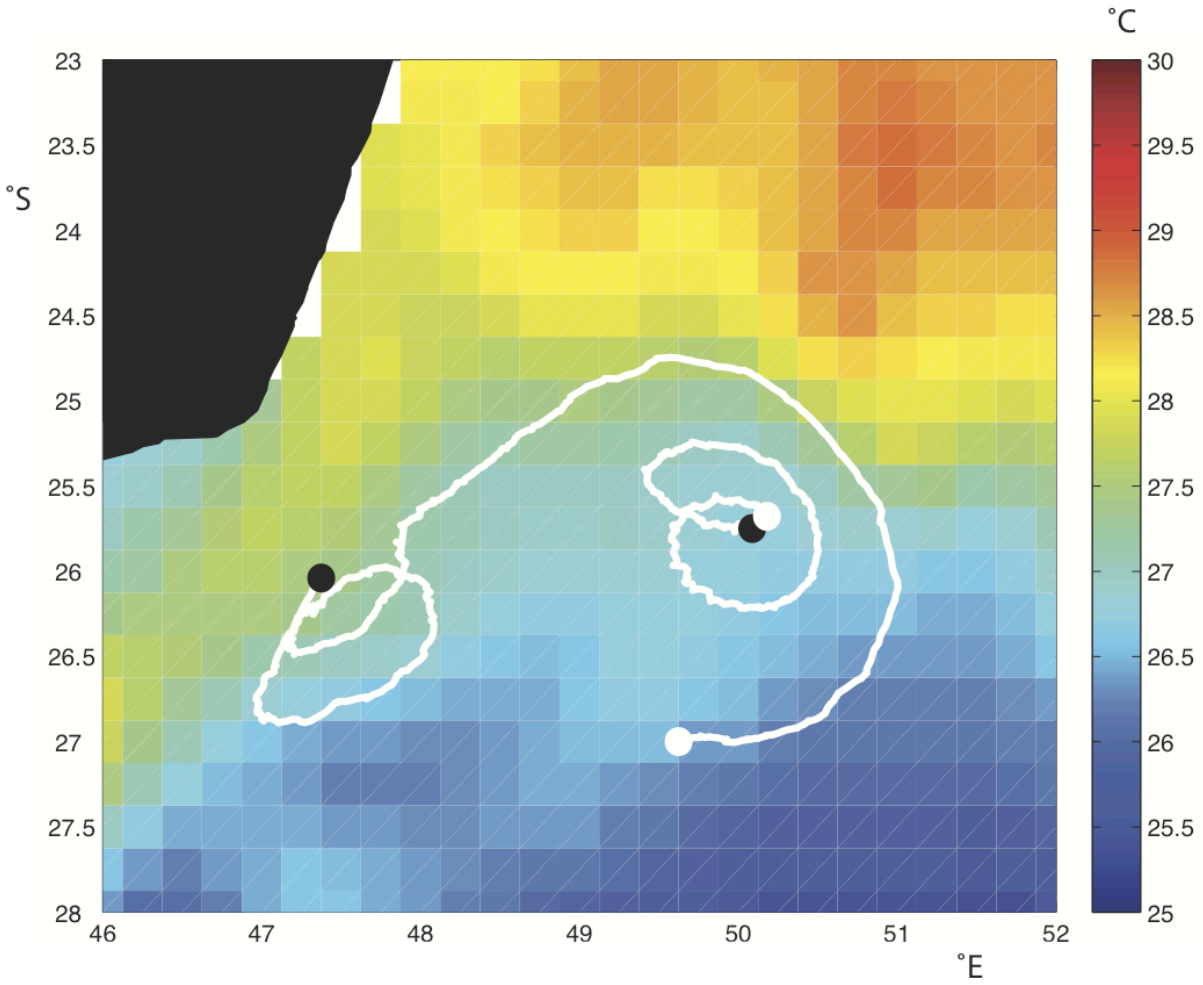

Figure 1c Level 4 sea surface temperature (SST) interpolated product for 15th February 2005. Image shown is the 0.25˚ product from NCDC based on optimal interpolation of AVHRR data [Reynolds et al., 2007]. Overlaid are the trajectories of two satellite-tracked surface drifters (details as for Figure 1a).

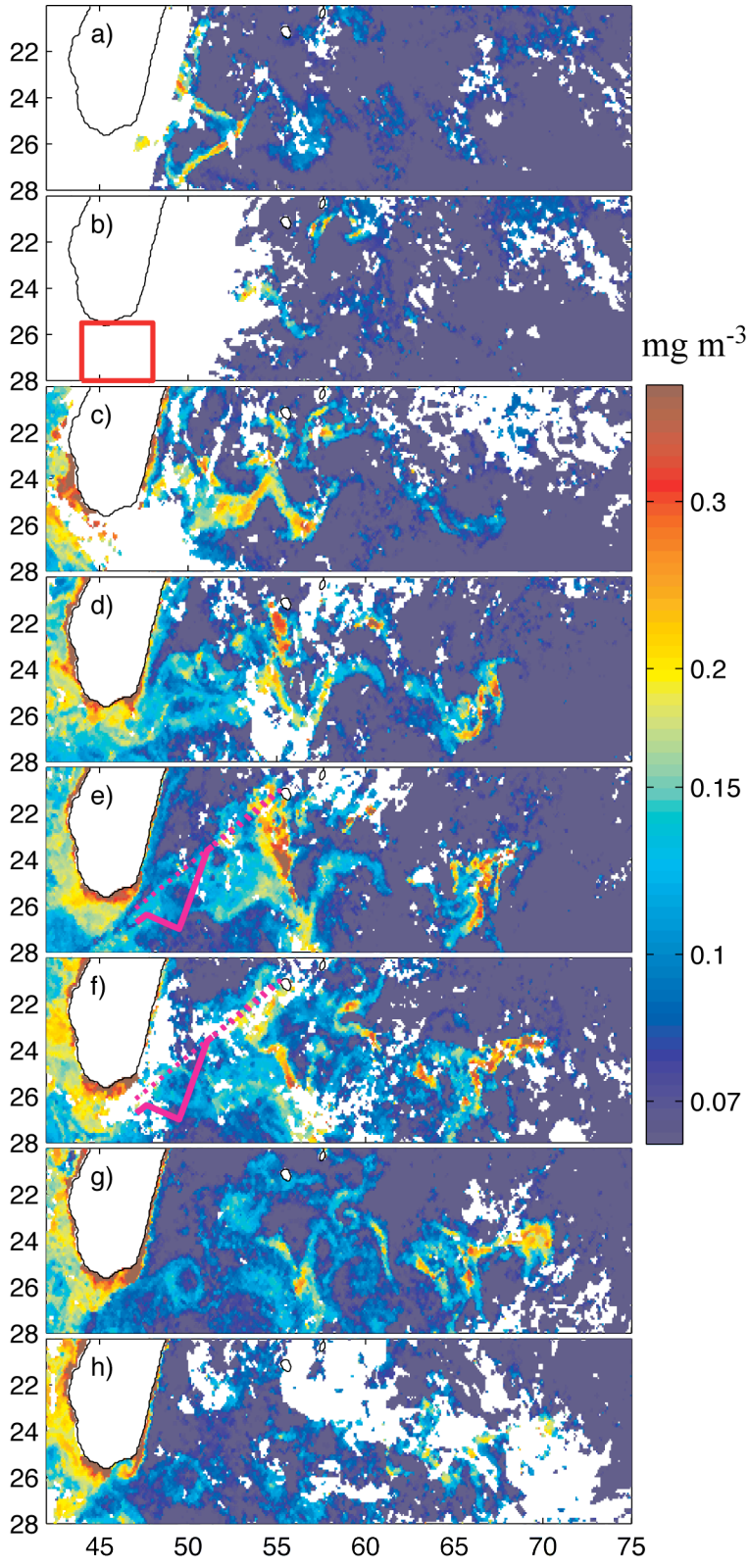

Figure 2 Sequence of SeaWiFS ocean color images (chlorophyll in mg m^{-3}) showing development of the bloom in 2005 – 7 day , with a 3 x 3 median spatial filter applied: a) 12-18 Jan; b) 19-25 Jan; c) 26 Jan – 1 Feb; d) 2-8 Feb; e) 9-15 Feb; f) 16-22 Feb; g) 23 Feb -1 Mar; h) 2-8 Mar. White areas are cloud covered. Red box in panel (b) denotes the main MadEx study region. On panels (e) and (f) the purple dotted line shows diversion to Réunion and the full purple line the track during SeaSoar deployment on return. The modulation of the bloom by the underlying mesoscale eddy field is clearly visible in the data. Note that the color scale differs from that in Figure 1a as the area shown is larger and the range of variability in chlorophyll is consequently greater.

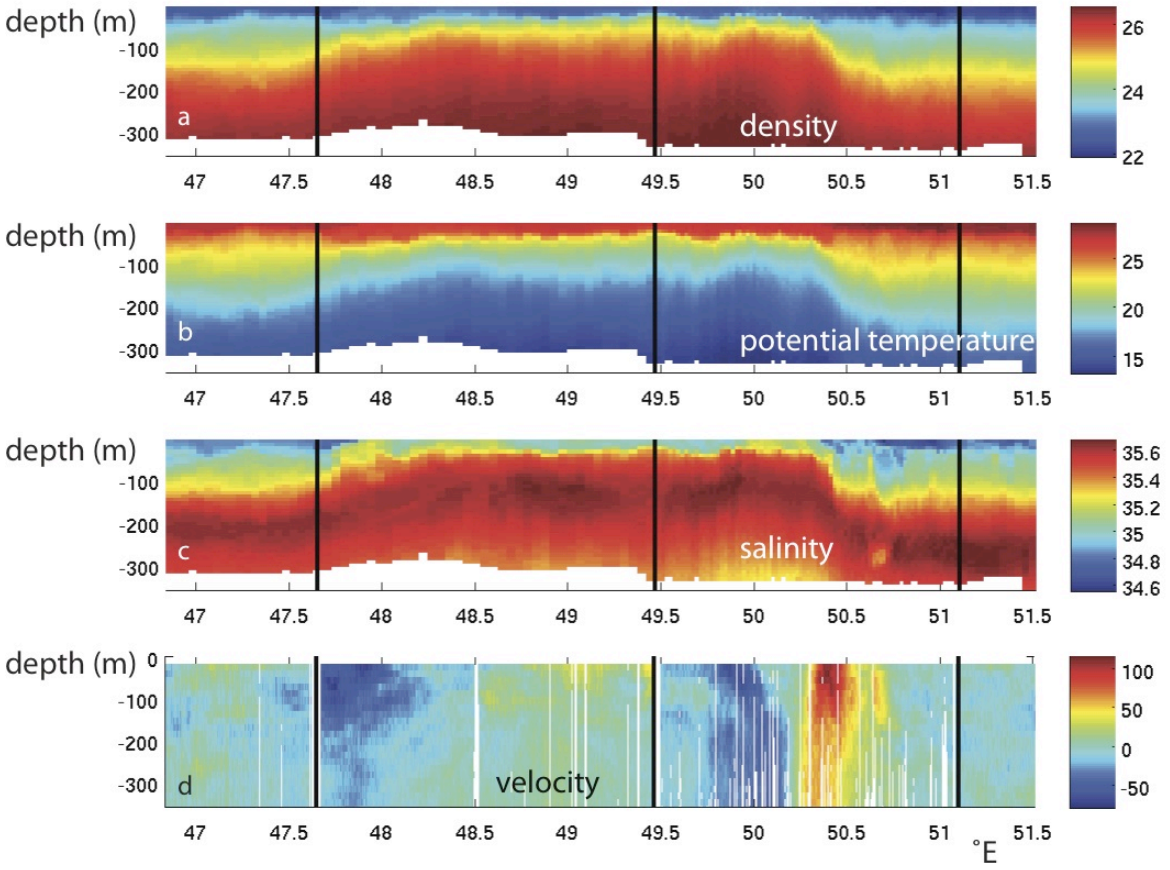

Figure 3 SeaSoar sections through bloom plotted against longitude. Top to bottom: a) density (kg m^{-3}), b) temperature (˚C), c) salinity, d) cross-track currents from 75 kHz ADCP (positive to left of track as ship travels southwest, cm s^{-1}). Note that hull-mounted ADCP does not make measurements in the top few meters. Vertical lines mark where the ship changes course (see Figure 1).

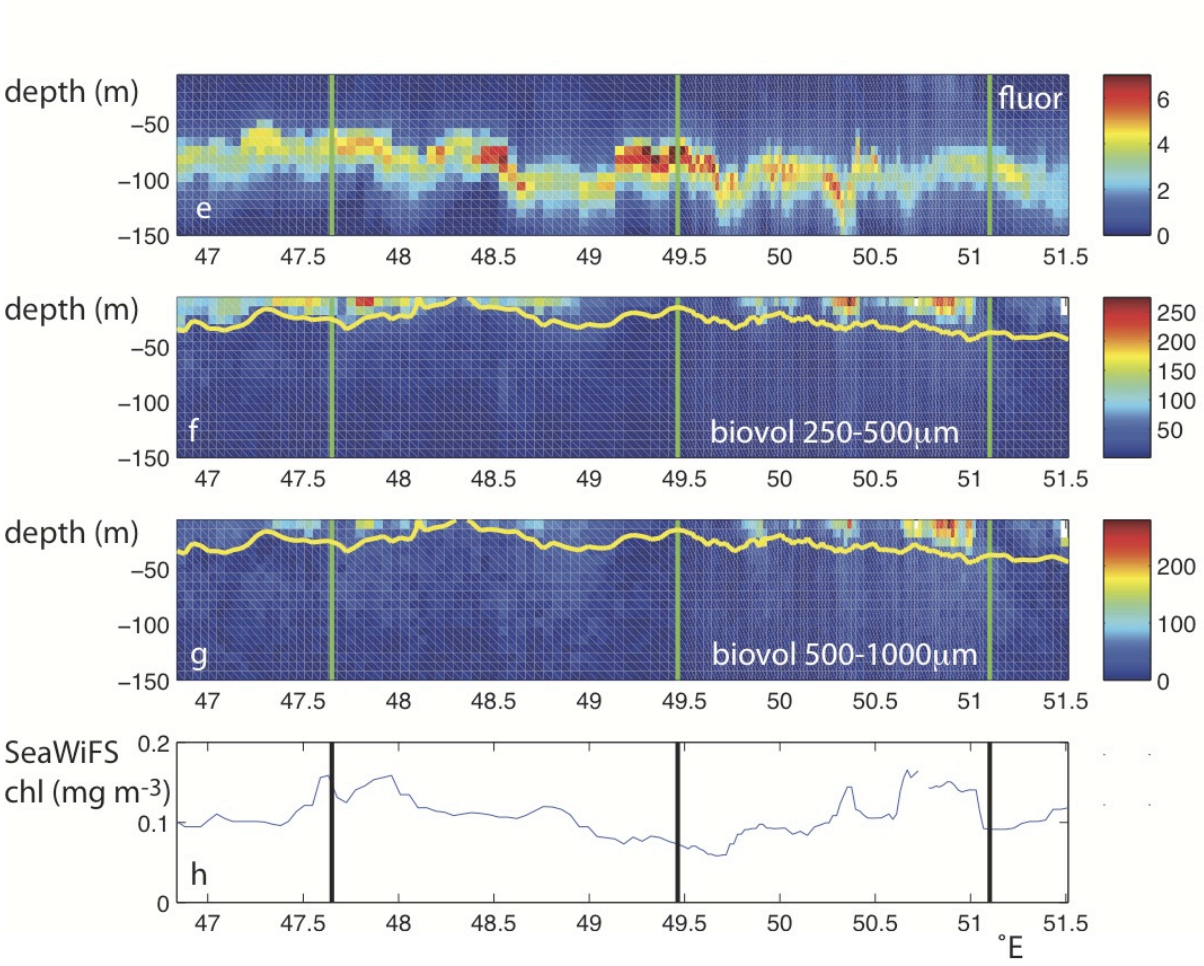

Figure 3 (continued) SeaSoar sections through bloom plotted against longitude. Top to bottom: e) chlorophyll fluorescence (mg m^{-3}), f) OPC biovolume in size class 250-500 µm, g) 500-1000 µm (mm^3 m^{-3}), h) SeaWiFS surface chlorophyll (mg m^{-3}). Vertical lines mark where the ship changes course (see Figure 1). The yellow contour in f & g is that for potential temperature equal to 26.5˚C. Note that chlorophyll fluorescence and OPC biovolume data are only shown for top 150 m. Vertical lines mark where the ship changes course (see Figure 1).

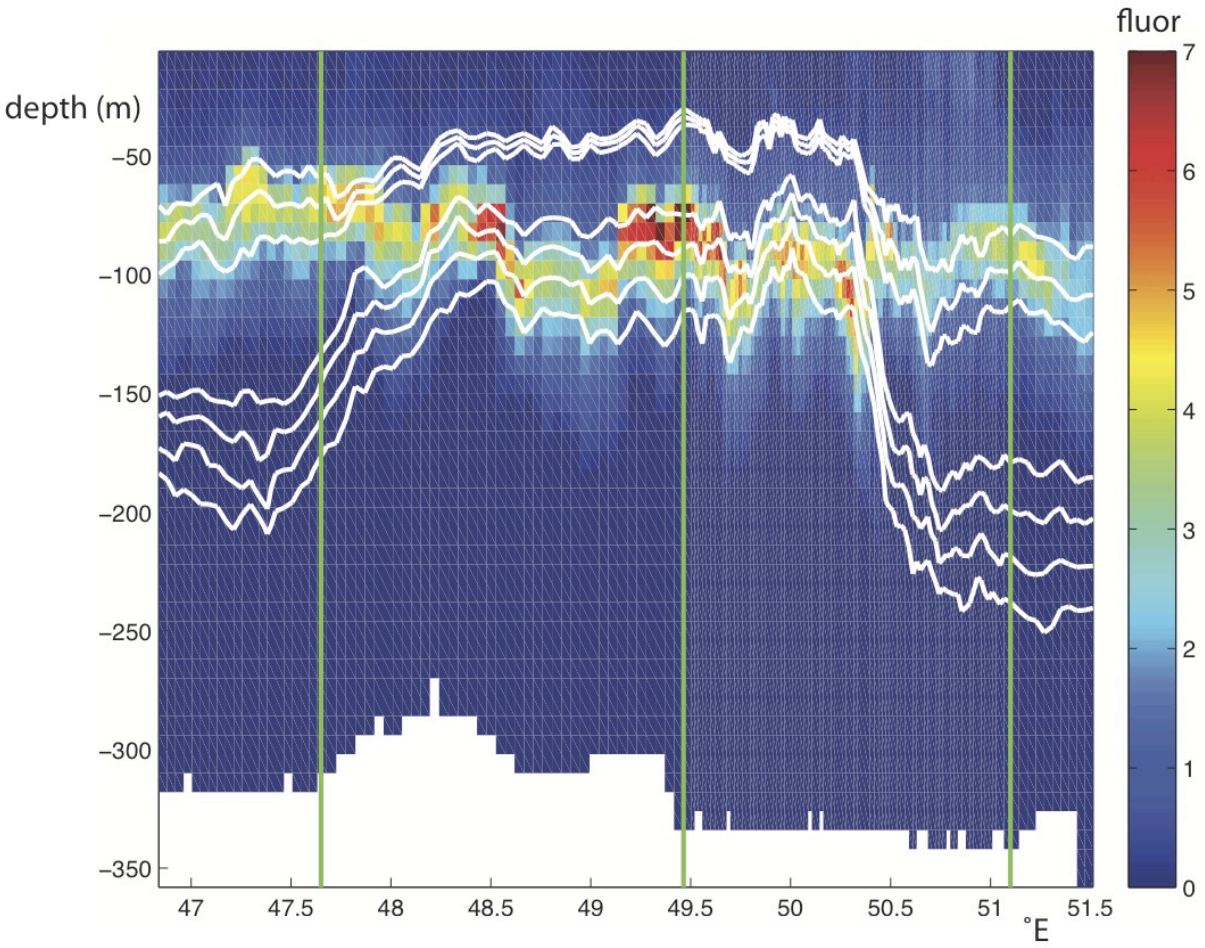

Figure 4 SeaSoar chlorophyll fluorescence data with density (kg m^{-3}) contours overlaid. Contours (shallowest to deepest) at 23.8, 24.0, 24.2, 25.0, 25.2, 25.4, 25.6 (kg m^{-3}). Vertical lines mark where the ship changes course (see Figure 1).

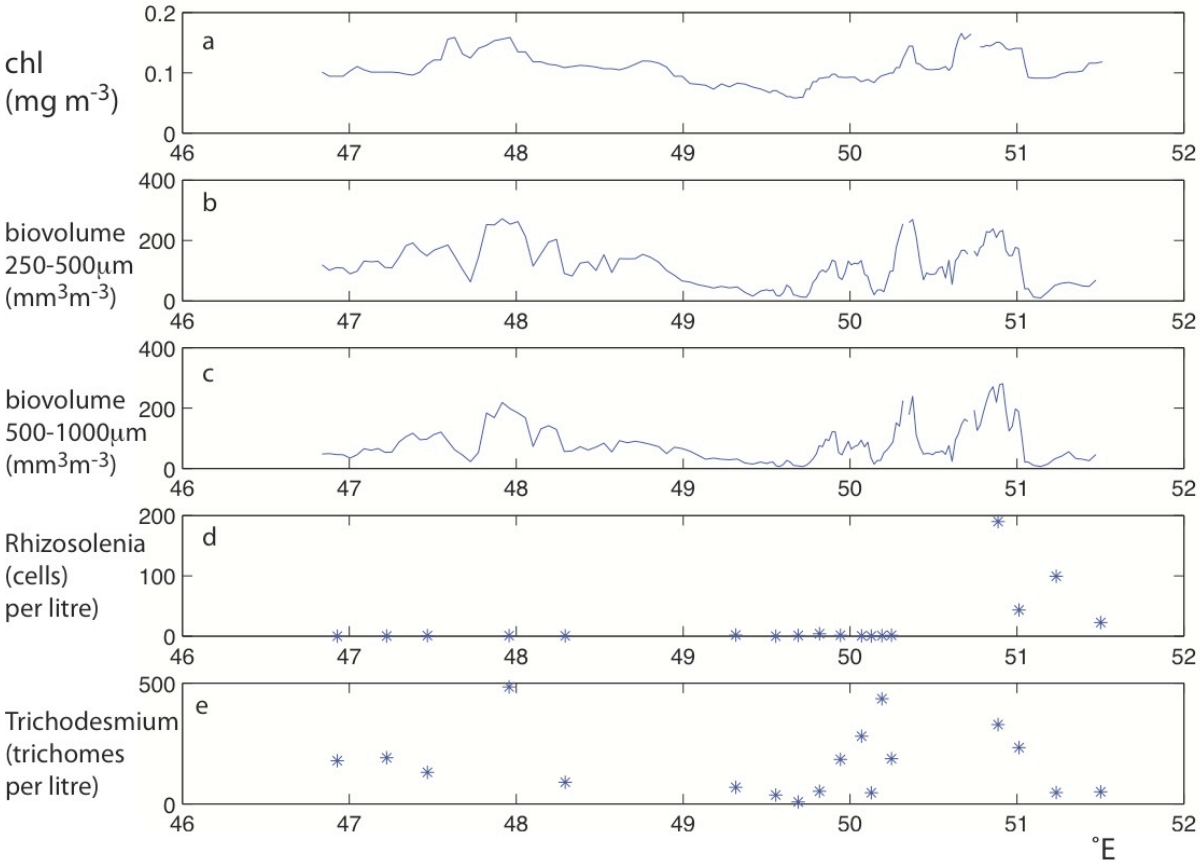

Figure 5 Surface values along SeaSoar transect of (top to bottom): a) SeaWiFS chlorophyll (mg m^{-3}), b) OPC biovolume in size class 250-500 μm (mm^3 m^{-3}), c) OPC biovolume in size class 500-1000 μm (mm^3 m^{-3}), d) *Rhizosolenia* abundance (cells per liter), e) *Trichodesmium* abundance (trichomes per liter).

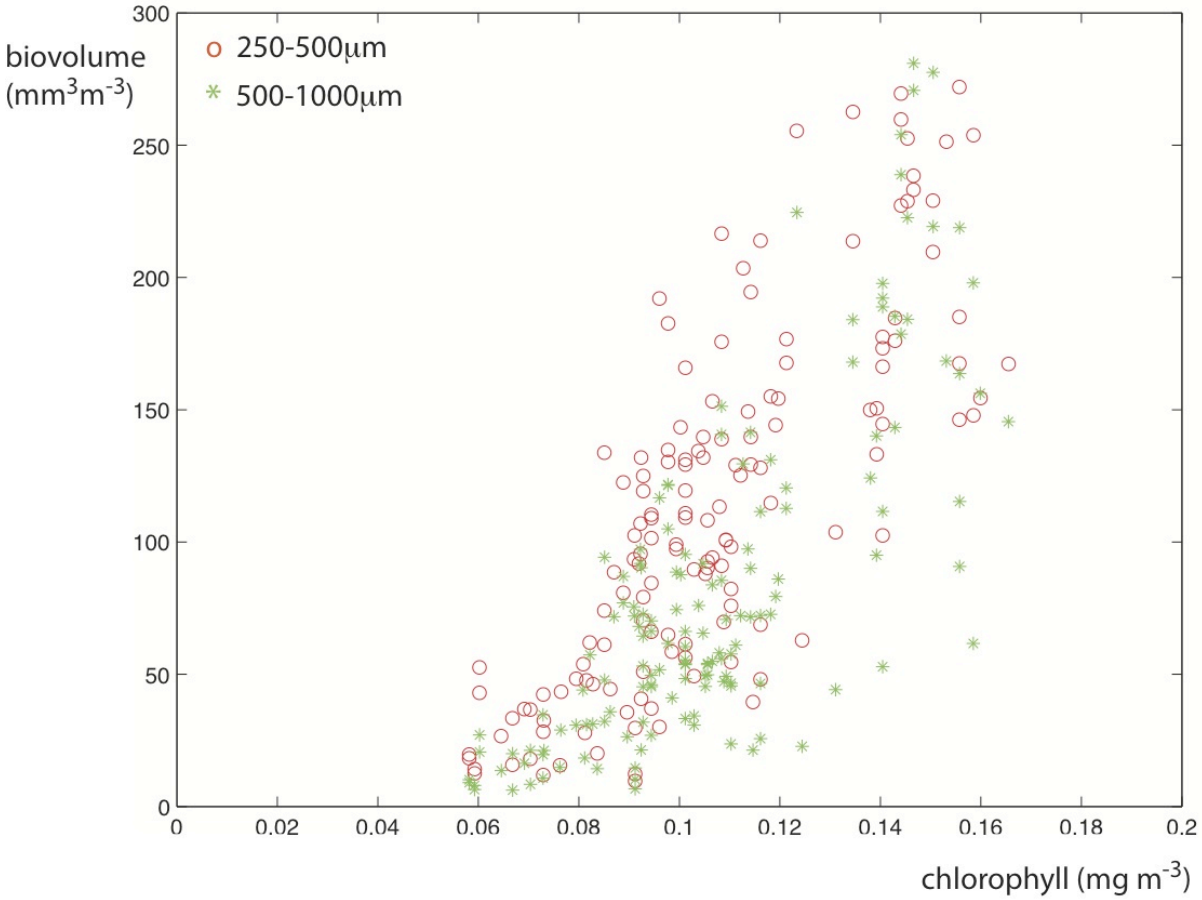

Figure 6 OPC biovolume in size classes 250-500 μm (red circles, mm^3 m^{-3}) and 500-1000 μm (green asterisks, mm^3 m^{-3}) plotted against SeaWiFS surface chlorophyll (mg m^{-3}).

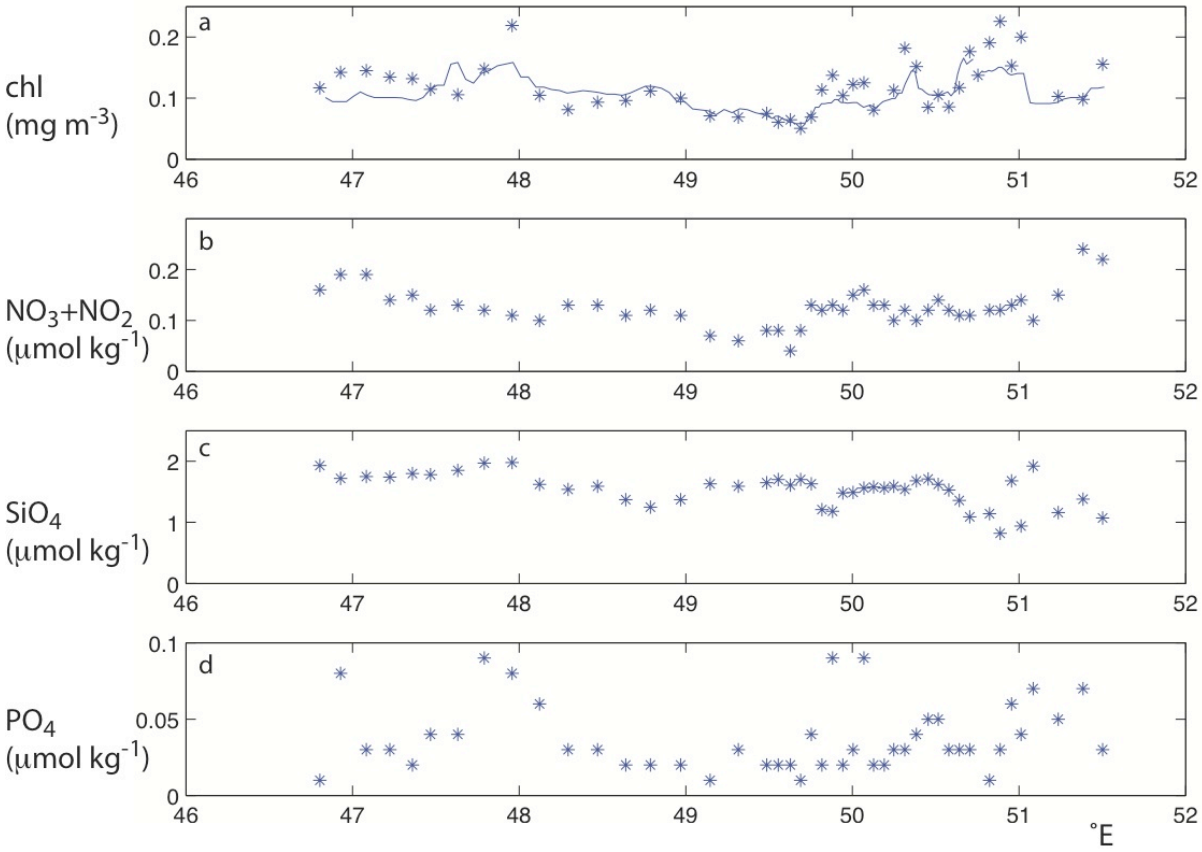

Figure 7 Surface values along SeaSoar transect of (top to bottom): a) SeaWiFS chlorophyll (mg m^{-3}) with *in situ* chlorophyll (*; mg m^{-3}), b) nitrate + nitrite (µmol kg^{-1}), c) silicate (µmol kg^{-1}), d) phosphate (µmol kg^{-1}).